Available online at www.sciencedirect.com

ScienceDirect

IFAC PapersOnline CONFERENCE PAPER ARCHIVE

IFAC PapersOnLine 55-41 (2022) 38–43

# Impact of VR Technology on a Human in Semi-autonomous Multi-robot Navigation: Control-Theoretic Perspective

**Takeshi Hatanaka** * **Takahiro Mochizuki** *
**Jose Maria Maestre Torreblanca** ** **Nikhil Chopra** ***

* *School of Engineering, Tokyo Institute of Technology, Tokyo 152-8552, Japan (e-mail: hatanaka@sc.e.titech.ac.jp; mochitaka@hfg.sc.e.titech.ac.jp).*
** *Systems and Automation Engineering Department, University of Seville, Spain (e-mail: pepemaestre@us.es)*
*** *Department of Mechanical Engineering, University of Maryland, USA (e-mail: nchopra@umd.edu)*

**Abstract:** In this paper, we investigate a scenario of one-human-multiple-robot navigation in three dimensions, and examine the impacts of the VR (Virtual Reality) technology on human properties from a control-theoretic perspective. We start by reviewing a passivity-based distributed control architecture that takes complementary interactions such that motion synchronization is autonomously completed by a distributed robot controller while the operator is dedicated to robot navigation. Due to the limited human capability of 3-D recognition and limited dimensionality on the real-time manipulability, 3-D navigation is completely different from that of the one- or two-dimensional case and we need to carefully design both feedback and command interfaces between the operator and robots. Specifically, we employ two different pairs of the interfaces, traditional joystick controller with 2-D display monitor and HMD (Head Mounted Display) with VR controller. We then build human models from the operation data with these interfaces on a human-in-the-loop simulator. Through the human modeling, we present two novel findings: (i) VR interfaces improve the accuracy of the human model with about 25∼45% of fitting ratio, which must drastically eases the design of human-robot collaboration systems, (ii) VR interfaces enhance human passivity, which is a key to ensuring closed-loop stability for the human-in-the-loop system.



*Keywords:* Distributed control, Mobile robots, Human–machine interface, Synchronization, System identification, Virtual reality, Passivity.

## 1. INTRODUCTION

Human-robot collaboration is a typical example of cyber-physical & human systems. The importance of the human model is indisputable for systematically designing a human-robot collaboration system. The right human model strongly depends on the role that the human plays in the system. Regarding the issue, Musić and Hirche (2017) classify the human role in the human-robot collaborations as either, active or supervisory, depending on the required level of autonomy. It is also pointed out by the authors that not only modeling of the human with supervisory role but also that with active role remain a largely open challenge. In this paper, we address modeling of the human with an active role, wherein the human mediacy ranges to the level of robot motion.

A promising approach to human-robot collaboration with the human active role lies in the celebrated paradigm of bilateral teleoperation (Hokayem and Spong, 2006; E. Nuño et al., 2011; Hatanaka et al., 2015). In this paradigm, the human operator is assumed to be a passive system, which allows rigorous theoretical guarantees on closed-loop stability. Beyond the traditional one-human-one-robot teleoperation, teaming between a human and multiple robots has been studied in depth, stimulated by the high maturity of distributed control technology for multi-robot systems. For example, teleoperation schemes for cooperative payload manipulation are reported in (Lee and Spong, 2005; Gioioso et al., 2014; Mohammadi et al., 2016; Staub et al., 2018), those for multi-robot navigation are presented in (Rodríguez-Seda et al., 2010; Franchi et al., 2012; Sabattini et al., 2012), and those for an exploration task are reported in (Li and Liu, 2019; Yang et al., 2021).

In this paper, we consider a scene of 3-D multi-robot navigation (Fig. 1). Regarding the problem, the authors presented a fully distributed control architecture based on passivity (Hatanaka et al., 2017; Atman et al., 2018), wherein the human passivity is a key in ensuring stability of the closed-loop system including the human. As a

⋆ Financial supports from Japan Society for the Promotion of Science (JSPS) KAKENHI (Grant 21K04104) and project C3PO-R2D2 (Grant PID2020-119476RB-I00 funded by MCIN/AEI/10.13039/501100011033) are gratefully acknowledged.


10.1016/j.ifacol.2023.01.100

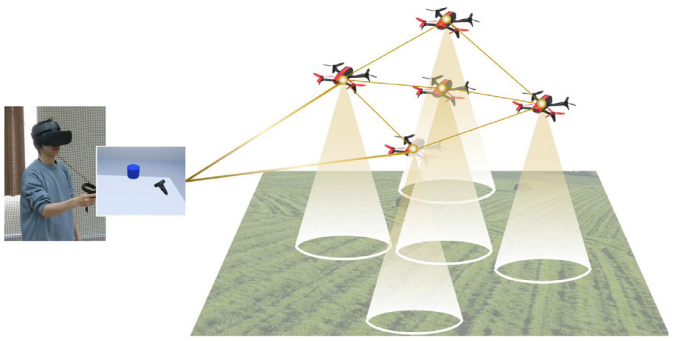

Fig. 1. A scene of 3-D one-human-multiple-robot collaboration.

remarkable difference from (Rodríguez-Seda et al., 2010; Franchi et al., 2012; Sabattini et al., 2012), we examined the human passivity through system identification techniques for the human operation data besides theoretical analysis. However, the data was collected on a 1-D human-in-the-loop simulator with a tablet as an interface. It remains unclear if the analytical results are applicable to the 3-D case. More specifically, due to the limited human capability of 3-D recognition and the limited dimensionality on the real-time manipulability, 3-D navigation may be completely different from that of the one- or two-dimensional cases, and we need to carefully design both feedback and command interfaces.

VR (Virtual Reality) technology is widely believed to enhance human 3-D recognition and manipulability. Indeed, many publications have been devoted to human-robot collaborations with VR devices as summarized in Dianatfar et al. (2021), wherein the effects of the VR technology on the human in various aspects have been examined. A missing piece of these works is analysis from control theoretic perspective. For example, the impact of VR interfaces on the human's dynamic behavior remains an open question. Moreover, to the best of the authors' knowledge, how it affects the human passivity has not been reported in the literature. This is the main focus of this paper.

In this paper, we analyze the impact of the VR technology on the human dynamic properties for the scenario of the multi-robot navigation in (Hatanaka et al., 2017). To this end, after reviewing (Hatanaka et al., 2017), we build a novel 3-D human-in-the-loop simulator with two different pairs of the interfaces, traditional joystick controller with 2-D display monitor and HMD (Head Mounted Display) with VR controller. We then build human models from the operation data on the simulator for appropriately arranged identification experiments. We then reveal the following two results: (i) VR interfaces improve the accuracy of the human model with about 25∼45% of fit ratio, and (ii) VR interfaces enhance the human passivity.

## 2. PRELIMINARY

Let us consider a dynamical system with the same input-output dimension whose state-space model is given as

$$\dot{x} = f(x) + g(x)u,\ x(0) = x_0, \tag{1a}$$
$$y = h(x), \tag{1b}$$

where $x \in \mathbb{R}^n$ is the state variable, $u \in \mathbb{R}^m$ is the control input, and $y \in \mathbb{R}^m$ is the system output. Suppose that there exists a positive semi-definite function $S : \mathbb{R}^n \to \mathbb{R}$ such that

$$S(x(\tau)) - S(x_0) \le \int_0^\tau y^T(t)u(t)dt$$

holds for all input signals, all initial states $x_0$, and all time $\tau \ge 0$. The system (1) is then said to be passive. If there exists $\delta \in \mathbb{R}$ such that

$$S(x(\tau)) - S(x_0) \le \int_0^\tau y^T(t)u(t)dt - \delta \int_0^\tau \|u(t)\|^2 dt$$

holds for all input signals, all initial states $x_0$, and all time $\tau \ge 0$, then the system is said to be input feedforward passive. The maximum of such $\delta$ is called input passivity index and is denoted by $\bar{\delta}$. If $\bar{\delta} \ge 0$, the system is passive.

Suppose now that (1) is a linear time-invariant system, and the transfer function matrix from $u$ to $y$ is denoted by $G(s)$. Define

$$\nu(\omega) = \lambda_{\min}(G(j\omega) + G^H(j\omega)),$$

where $\lambda_{\min}(A)$ is the minimal eigenvalue of the matrix $A$. Then, it is well known that $\bar{\delta} = \min_\omega \nu(\omega)$ holds (Qu and Simaan, 2014). The function $\nu(\omega)$ is thus regarded as a passivity metric corresponding to angular frequency $\omega$.

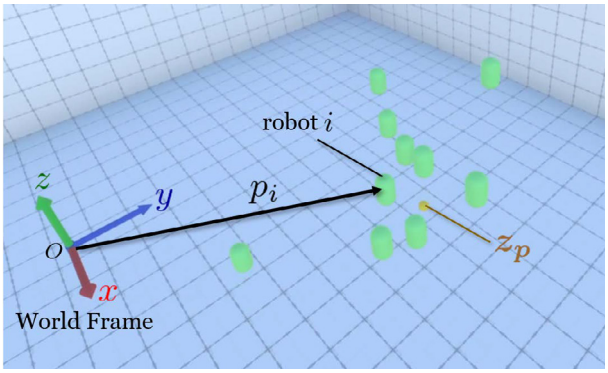


Fig. 2. A scene of 3-D human-multiple-robot collaboration.

## 3. SYSTEM ARCHITECTURE

In this section, we briefly review the formulation of (Hatanaka et al., 2017) as it is directly applicable to the 3-dimensional case.

We consider a group of $n$ robots with the set of their IDs $\mathcal{V} = \{1, 2, \ldots, n\}$ in 3-D Euclidean space as illustrated in Fig. 2. The position of robot $i$ relative to the world frame $\Sigma_w$ is denoted by $p_i \in \mathbb{R}^3$. Throughout this paper, we assume that the motion of robot $i$ is modelled by a single integrator

$$\dot{p}_i = u_i, \tag{2}$$

where $u_i \in \mathbb{R}^3$ is the velocity input to be designed.

Suppose that the above robots are able to exchange information through a network modelled by an undirected graph $G = (\mathcal{V}, \mathcal{E})$, $\mathcal{E} \subseteq \mathcal{V} \times \mathcal{V}$. The set of neighbor set $\mathcal{N}_i$ is defined as $\mathcal{N}_i = \{j \in \mathcal{V} |\ (i, j) \in \mathcal{E}\}$. In the sequel, we assume that the graph is fixed and connected.

Let us now consider a human operator whose role is to drive all robots to a desirable position $r_p$ or velocity $r_v$. The operator has a feedback interface and a command interface to interact with the robot, where the former

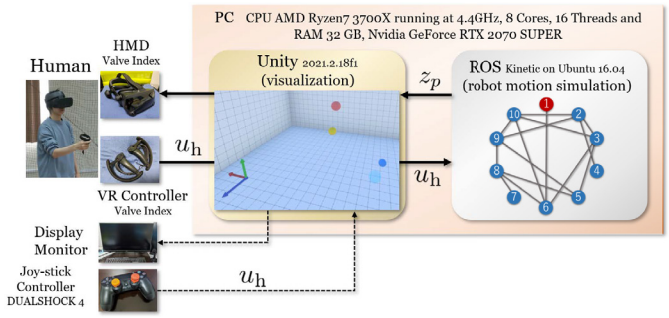


Fig. 3. Schematic of 3-D human-in-the-loop simulator.

translates the output of the robotic group to visual feedback information for the operator and the latter translates the human action to a control command for the robot group. We suppose that both interfaces have access to a subset of robots $\mathcal{V}_h \subseteq \mathcal{V}$ by wireless communication.

The control goals addressed in Hatanaka et al. (2017) are described as below. The operator first chooses the quantity to control between robot positions and velocities. If the operator wishes to control robot positions, the goal is formulated by

$$\lim_{t\to\infty} \|p_i - r_p\| = 0 \ \forall i \in \mathcal{V}. \tag{3}$$

In the case of the velocity navigation, it is by

$$\lim_{t\to\infty} \|\dot{p}_i - r_v\| = 0 \ \forall i \in \mathcal{V}, \tag{4a}$$

$$\lim_{t\to\infty} \|p_i - p_j\| = 0 \ \forall i, j \in \mathcal{V}. \tag{4b}$$

In order to achieve the above control goals, Hatanaka et al. (2017) presented a distributed controller based on so-called PI consensus algorithm.

$$u_i = \sum_{j\in\mathcal{N}_i} a_{ij}(p_j - p_i) + \sum_{j\in\mathcal{N}_i} b_{ij}(\xi_i - \xi_j) + \delta_i u_h \tag{5a}$$

$$\dot{\xi}_i = \sum_{j\in\mathcal{N}_i} b_{ij}(p_j - p_i), \tag{5b}$$

where $a_{ij}$ and $b_{ij}$ are positive scalars, and $\delta_i = 1$ if $i \in \mathcal{V}_h$ and $\delta_i = 0$ otherwise. The signal $u_h$ is the velocity command determined by the human operator. Hatanaka et al. (2017) further revealed that the collective dynamics (2) with (5) for all $i \in \mathcal{V}_h$ is passive from $u_h$ to $z_p$ and $\dot{u}_h$ to $z_v$ respectively, where $z_p$ and $z_v$ are average position and velocity among robots in $\mathcal{V}_h$, namely

$$z_p = \frac{1}{|\mathcal{V}_h|}\sum_{i\in\mathcal{V}_h} p_i, \ \ z_v = \frac{1}{|\mathcal{V}_h|}\sum_{i\in\mathcal{V}_h} \dot{p}_i. \tag{6}$$

Remark that differentiability of $u_h$ is ensured by applying a filter to the raw command signal by the operator in the architecture of (Hatanaka et al., 2017).

Based on the passivity paradigm, we feed $z_p$ or $z_v$ back to the operator, where the signals are switched at the feedback interface depending on the selected control goal. Hatanaka et al. (2017) then proved that either of (3) and (4) with constant references $r_p$ and $r_v$ is achieved under human passivity together with additional assumptions, even without sharing the selected control goal among the robots. Hatanaka et al. (2017) further examined human passivity through system identification techniques for the operation data on a 1-D human-in-the-loop simulator.

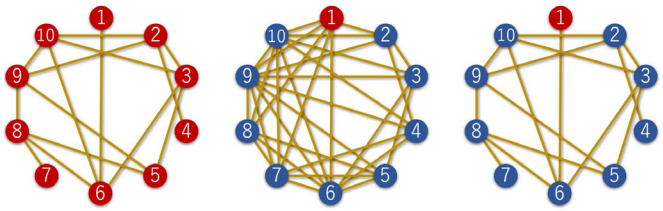

Fig. 4. Communication networks, where the red nodes belong to $\mathcal{V}_h$ and the blue do not.

The above paper treated planar robots but the mathematical proofs are directly applied to 3-D case. However, it is not trivial to determine whether the human operator behaves in the same way as 1-D and 2-D operations mainly due to the limited human capability of 3-D recognition and higher dimensionality of manipulated variables. This is the main issue to be addressed in this paper. It is now to be noted that a dominant factor to determine the human behavior is the interface. More specifically, VR technology is expected to enhance the human recognition and manipulation but its impact from control theoretic perspectives including passivity has not been well analyzed.

## 4. SIMULATION ENVIRONMENT AND IDENTIFICATION EXPERIMENTS

In this section, we present a human-in-the-loop simulator and the identification experiments to collect the operation data for modeling and analyzing the human properties. In the sequel, we address only position navigation while leaving velocity navigation to future work.

### *4.1 Human-in-the-loop Simulator*

We built a human-in-the-loop simulator illustrated in Fig. 3. In the simulator, we employ 10 robots with three different types of networks in Fig. 4. In Type 1 (left), the inter-robot network is sparse but all robots are connected to the operator. In Type 2 (middle), the inter-robot network is dense, but only robot 1 is connected to the operator. In Type 3 (right), the inter-robot network is the same as Type 1, but only robot 1 is connected to the operator. The robot motion dynamics (2) and (5) is simulated on ROS (Robot Operating System) in anticipation of future expansion into robotic experiments. The average information $z_p$ is sent to Unity that generates 3-D graphics to smoothen the interactions between the human and robots in three dimensions.

We prepare two pairs of feedback and command interfaces. The first one is the pair of a standard gaming-type joystick-based controller, DUALSHOCK 4(Sony Corp.), and 2-D 27-inch display monitor. The left stick specifies the $x$- and $z$-coordinates of the command $u_h$, while the longitudinal operation of the right stick corresponds to the $y$-coordinate. We tuned the gain from the joystick angle to $u_h$ so that the maximal angle corresponds to $\pm 0.15$m/s for Type 1 and $\pm 1.5$m/s for Type 2 and 3 in view of the human operability and the fact that the stationary gain from $u_h$ to $z_p$ for Type 1 is 10 times as large as those for Type 2 and 3 (Hatanaka et al., 2017). Remark that the relative stationary gain is simply determined by $|\mathcal{V}_h|/n$ and it is reasonable to change the gain at the interface

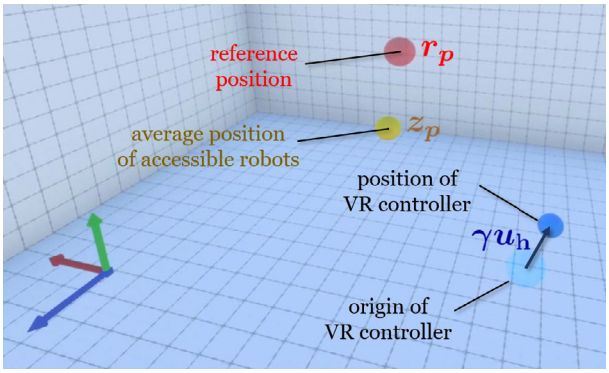


Fig. 5. A scene viewed during the operation.

Table 1. Interface selections in the identification experiments.

| | feedback interface | command interface |
|---|---|---|
| case 1 | 2-D display | joystick |
| case 2 | HMD | VR controller |
| case 3 | 2-D display | VR controller |

depending on the network structure. The command signal $u_\mathrm{h}$ is then directly sent to a topic and ROS subscribes and substitutes the signal into $u_\mathrm{h}$ in (5). The 3-D graphics generated by Unity is displayed on the monitor, where the viewpoint is fixed and viewing angle is set to 60deg throughout experiments. In this setting, there is a risk that robots may get out of the field of view, but we arranged the experiments so that it does not happen since this issue is beyond the scope of this work.

The second pair of the interface is the VR interface, Valve Index VR (Valve Corp.), consisting of an HMD and VR controller. These devices are connected to Unity and the HMD receives and displays the 3-D graphics, where the viewing angle varies depending on the attitudes of the human head. The operator initially pushes a button of the controller and the location of the controller at this moment is set to the origin, which is also displayed on the HMD with a cyan ball as shown in Fig. 5. The blue ball indicates the current position of the controller and the vector from the origin to the real-time position of the VR controller is converted to $\gamma u_\mathrm{h}$ and is sent to ROS through Unity. The parameter $\gamma$ is selected as 2 for Type 1 and 0.2 for Type 2 and 3 so that larger signals can be commanded by the operator for Type 2 and 3. In the real operation, the human hand motion in each coordinate is almost limited to $\pm$30cm, and $\|u_\mathrm{h}\|_\infty$ is approximately restricted to 0.15m/s for Type 1 and 1.5m/s for Type 2 and 3 in the same way as above. The average position $z_p$ of the robots in $\mathcal{V}_\mathrm{h}$ is displayed as the yellow ball in Fig. 5.

### *4.2 Design of Identification Experiments*

Let us next design identification experiments on the above simulator. The trial subject is told to drive the average position (yellow ball) to a reference position (red ball) so that the yellow one with diameter 5cm eventually lies inside of the red with diameter 5.5cm through operating the joysticks or the VR controller. The reference randomly jumps at every 15s to a point in a cube of side 2m including the operator whose center is located at height 1m from the floor. The interval of the jumps is determined so that the operator can almost complete the settling of the yellow to the red for all network types. One trial consists of 10 jumps of the reference and it takes 150s in total.

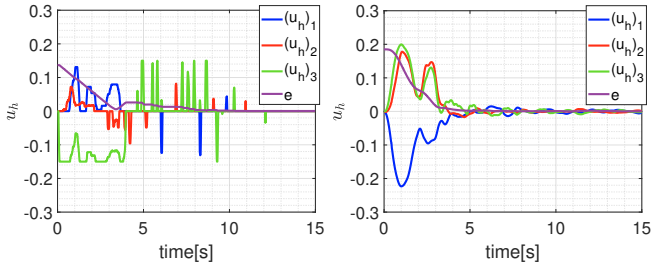


Fig. 6. Time series data of $u_\mathrm{h}$ for the joystick (left) and VR controller (right), where the purple curve shows the error $e = r_p - z_p$.

After completing a certain amount of training for the system operation, the operator conducts trials for all network types in Fig. 4 under the three different interface settings in Table 1. The sampling period of the data was not stable but it was about 0.0083s on average. We take this average in the system identification of the human operator. It is also to be noted that we add an additional process to the acquired data in the same way as (Hatanaka et al., 2017). Namely, the subject is told to push a button when he/she recognizes new references and starts operation. The data is then shifted so that the initial time of the operation synchronizes the time of pushing the button, which excludes the delays just for recognizing the new references. The reference is generated by the operator in the real operation, and the recognition delay is a phenomenon unique to this experiment.

The time series data of the command $u_\mathrm{h}$ over 15s for the joystick and VR controller are illustrated in the left and right plots of Fig. 6, respectively. We see from the data that the operator with the joystick tends to take extreme actions because the spring built into the stick makes fine manipulation difficult. This is why the operator inputs large values at short intervals even in the settling phase with a small error. On the other hand, it is observed that the command by the VR controller is much smoother than that for the joystick.

## 5. RESULTS AND DISCUSSIONS

### *5.1 Model Accuracy*

We build the human operator model using MATLAB System Identification Toolbox (Mathworks Inc.) and the so-called direct approach to the closed-loop system identification (Katayama, 2010) for the data of one trial in case 1 and 2. We employed the option of the continuous-time model. The model order is empirically determined based on the fit ratio as two poles and one zero for all elements of the transfer function matrix. We tested a variety of other settings, but could not achieve a better fit than this setting. The time responses of the model outputs and the identification data for Type 1 network are illustrated in Fig. 7. We see from the figures that the extreme actions of the joystick in the left plot cannot be identified, whereas the smooth data for the VR controller are almost correctly fitted. In particular, a remarkable feature is found in the

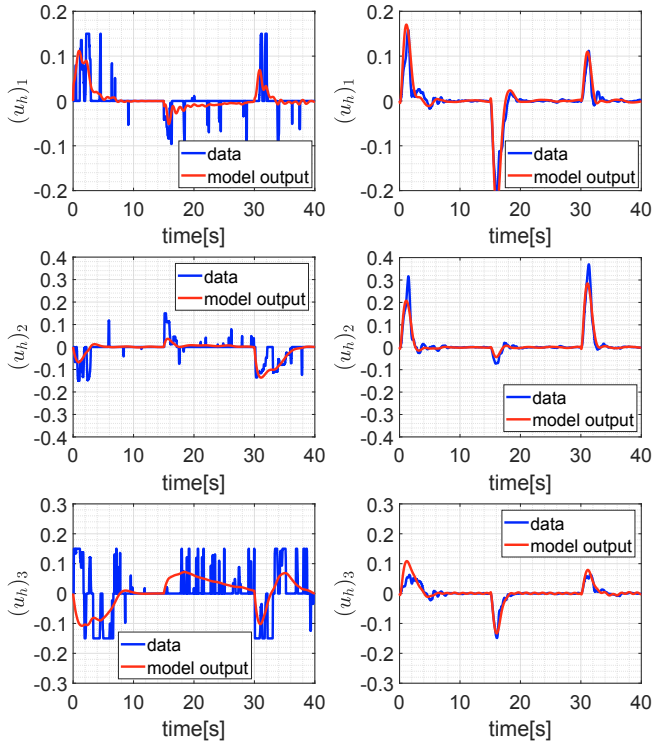


Fig. 7. Time responses of the model outputs (red) and the identification data (blue) on $u_\mathrm{h}$ for Type 1 network (left: case 1, right: case 2).

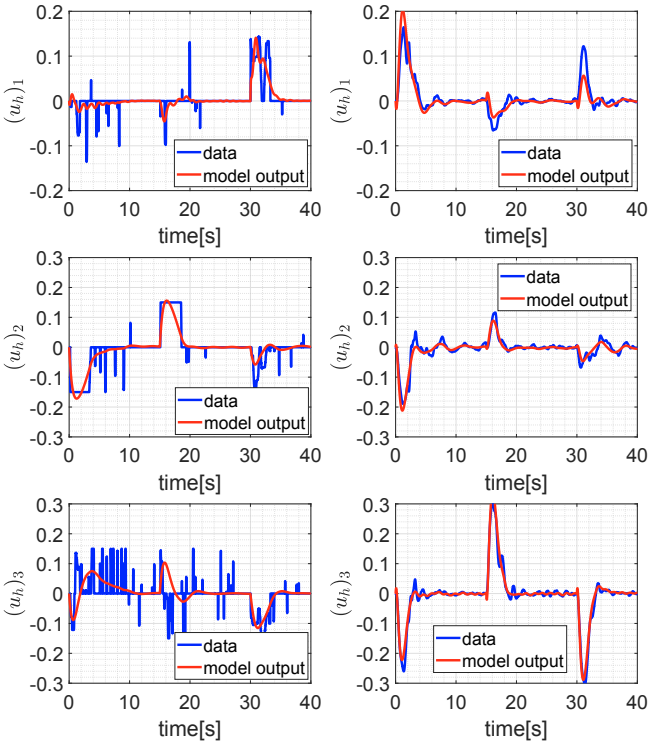


Fig. 8. Time responses of the model outputs (red) and the verification data (blue) on $u_\mathrm{h}$ for Type 1 network (left: case 1, right: case 2).

Table 2. Average model fit ratios among three elements of $u_\mathrm{h}$ for the identification data

| | Type 1 | Type 2 | Type 3 |
|---|---|---|---|
| case 1 | 38.64% | 40.82% | 37.93% |
| case 2 | 68.88% | 56.26% | 78.76% |
| case 3 | 50.03% | 44.79% | 55.37% |

Table 3. Average model fit ratios among three elements of $u_\mathrm{h}$ for the verification data

| | Type 1 | Type 2 | Type 3 |
|---|---|---|---|
| case 1 | 32.45% | 19.21% | 19.68% |
| case 2 | 71.19% | 54.50% | 66.42% |
| case 3 | 34.79% | 28.59% | 28.72% |

bottom left figure whose coordinate corresponds to the depth from the viewpoint. Due to the limited capability of the depth recognition from 2-D images, the model accuracy for this coordinate is considerably worse than the above two, whereas the model for the VR interface almost correctly fits the data for all coordinates. The same was applied to case 3. The fit ratios for the three network types are summarized in Table 2. It is confirmed that the models for the VR interface fit the data more accurately than those for the traditional interface.

We next conduct the cross validation by taking the data for another trial as verification data. Fig. 8 illustrates the time responses of the model outputs and the verification data for Type 1 network. It is recognized even visually that the fitting performance degrades as compared with Fig. 8, but the model for the VR interface fits the data more accurately than that for the traditional one. It is also confirmed from the fit ratios for various networks in Table 3 that the VR interfaces improve the model accuracy with 25∼45% as compared with the other cases.

In summary, it is concluded that the VR interface simplifies the human behavior to the extent that it can be represented by a simple linear time invariant system. This drastically reduces the human uncertainty in the loop and simplifies the design of cyber-physical and human systems.

### *5.2 Human Passivity*

In this subsection, we examine the impact of the VR interface on the human passivity. Since the model for case 1 is not always accurate enough to discuss the passivity, we take the model for case 3 as a comparison with the model for case 2. This means that we analyze how the higher 3-D recognition ability brought by the HMD enhances the human passivity.

Fig. 9 illustrates the passivity index $\nu(j\omega)$ for the three networks, where the blue and red curves show the index for the model in case 1 and that in case 3, respectively. See (Hatanaka et al., 2017) for the explanation of the limited frequency domain in the figures. It is immediately observed that the index for the model with the HMD almost takes larger values than that for the 2-D display. In other words, the HMD improves the human passivity, which implies that stability of the human-in-the-loop system is enhanced by the VR device. On the other hand, these figures indicate that the human operator is not passive for all networks regardless of the interface even if we ignore the notches stemming from overfitting. This motivates us to take the architecture in (Atman et al., 2018), which allows the passivity shortage of the human operator.

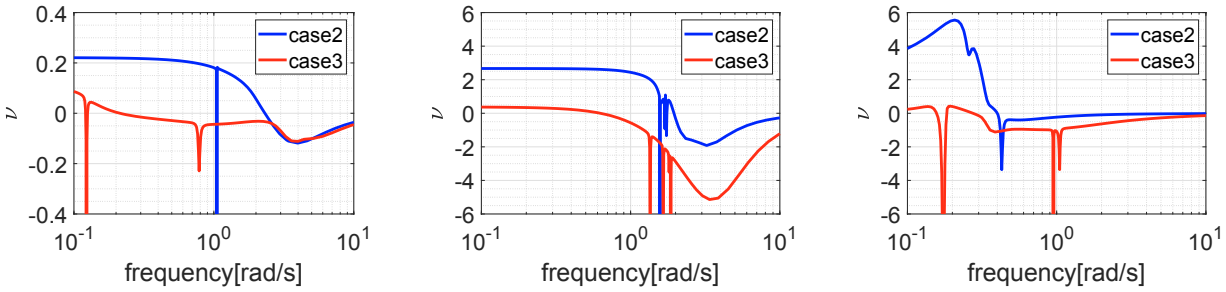


Fig. 9. Passivity index $\nu$ for Type 1 (left), Type 2 (middle), and Type 3 (right).

## 6. CONCLUSION

In this paper, we examined the impact of VR technology on the human in a semi-autonomous multi-robot navigation system. In particular, the VR interface is shown to reduce the model complexity of the human and to enhance human passivity. The quantitative results are unique to the specific architecture, but they would be qualitatively applied to other control architectures at least from the smooth curves in the right of Fig. 6.

This paper presents just a first trial and many issues remain open. As described in the end of Section 5.2, it is indispensable to test the architecture in (Atman et al., 2018). Passivity analysis for the velocity navigation has also to be performed. We also have to analyze how the VR interface affects the human workload, e.g., through the NASA TLX questionnaire, as done in (Atman et al., 2018). The VR interface opens the door for the extension to full 3-D rigid-body motion including attitude dynamics, which should be addressed in the future.

## REFERENCES

S. Musić and S. Hirche. Control sharing in human-robot team interaction. Annual Reviews in Control, vol. 44, pages 342–354, 2017.

P.F. Hokayem and M.W. Spong. Bilateral teleoperation: A historical survey. Automatica, vol. 42, no. 12, pages 2035–2057, 2006.

E. Nuño, L. Basañez, and R. Ortega. Passivity-based control for bilateral teleoperation: A tutorial. Automatica, vol. 47, no. 3, pages 485–495, 2011.

T. Hatanaka, N. Chopra, M. Fujita, and M.W. Spong. *Passivity-Based Control and Estimation in Networked Robotics*. Springer-Verlag, 2015.

D. Lee and M.W. Spong. Bilateral teleoperation of multiple cooperative robots over delayed communication network: Theory. In 2005 IEEE International Conference on Robotics and Automation, pages 360–365, 2005.

G. Gioioso, A. Franchi, G. Salvietti, S. Scheggi, and D. Prattichizzo. The flying hand: A formation of uavs for cooperative aerial tele-manipulation. In 2014 IEEE International Conference on Robotics and Automation, pages 4335–4341, 2014.

M. Mohammadi, A. Franchi, D. Barcelli, and D. Prattichizzo. Cooperative aerial tele-manipulation with haptic feedback. In 2016 IEEE/RSJ International Conference on Intelligent Robots and Systems, pages 5092–5098, 2016.

N. Staub, M. Mohammadi, D. Bicego, Q. Delamare, H. Yang, D. Prattichizzo, P.R. Giordano, D. Lee, and A. Franchi. The tele-magmas: An aerial-ground comanipulator system. IEEE Robotics and Automation Magazine, vol. 25, no. 4, pages 66–75, 2018.

E.J. Rodríguez-Seda, J.J. Troy, C.A. Erignac, P. Murray, D.M. Stipanovic, and M.W. Spong. Bilateral teleoperation of multiple mobile agents: Coordinated motion and collision avoidance. IEEE Transactions on Control Systems Technology, vol. 18, no. 4, pages 984–992, 2010.

A. Franchi, C. Secchi, H.I. Son, H.H. Bulthoff, and P.R. Giordano. Bilateral teleoperation of groups of mobile robots with time-varying topology. IEEE Transactions on Robotics, vol. 28, no. 5, pages 1019–1033, 2012.

L. Sabattini, B. Capelli, C. Fantuzzi, and C. Secchi. Teleoperation of multi-robot systems to relax topological constraints. In Proc. 2020 IEEE International Conference on Robotics and Automation, pages 4558–4564, 2020.

W.-T. Li and Y.-C. Liu. Human-swarm collaboration with coverage control under nonidentical and limited sensory range. Journal of the Franklin Institute, vol. 356, no. 16, pages 9122–9151, 2019.

Y. Yang, D. Constantinescu, and Y. Shi. Proportional and reachable cluster teleoperation of a distributed multi-robot system. In Proc. 2021 IEEE International Conference on Robotics and Automation, pages 8984–8990, 2020.

L. Sabattini, B. Capelli, C. Fantuzzi, and C. Secchi. Teleoperation of multi-robot systems to relax topological constraints. In Proc. 2020 IEEE International Conference on Robotics and Automation, pages 4558–4564, 2020.

T. Hatanaka, N. Chopra, J. Yamauchi, and M. Fujita. A passivity-based approach to human-swarm collaborations and passivity analysis of human operators. In Y. Wang and F. Zhang, editors, *Trends in Control and Decision-Making for Human-Robot Collaboration Systems*, pages 325–355. Springer-Verlag, 2017.

M. W. S. Atman, K. Noda, R. Funada, J. Yamauchi, T. Hatanaka and M. Fujita. On passivity-shortage of human operators for a class of semi-autonomous robotic swarms. In Proc. 2nd IFAC Conference on Cyber-Physical & Human Systems, pages 21–27, 2018.

M. Dianatfar, J. Latokartano, and M. Lanz. Review on existing VR/AR solutions in human–robot collaboration. Procedia CIRP, vol. 97, pages 407-411, 2021.

Z. Qu and M.A. Simaan. Modularized design for cooperative control and plugand- play operation of networked heterogeneous systems. Automatica, vol. 50, no. 9, pages 2405–2414, 2014.

T. Katayama. Subspace Methods for System Identification. Springer-Verlag, Switzerland, 2010.